

# INVESTIGATION OF PORE SIZE AND RESIN ABSORBENCY IN CHOPPED STRAND MATS

Zoltán GOMBOS, Veronika NAGY, László Mihály VAS, János GAÁL

Department of Polymer Engineering,  
Budapest University of Technology and Economics  
H-1111 Budapest, Műegyetem rkp. 3., Hungary

Received: January 24, 2005

## Abstract

The main aim was to measure and evaluate the absorption ability of resins in glass fiber mats most often used in Hungary since pore size influences the absorbance process and the absorbed quantity of resin during composite production when the resin is still in a liquid phase. The average value of pores and their distribution function were estimated using the mat statistic model and the measured geometrical parameters. The measurement and evaluation method developed can be used to model the liquid absorbance process of glass fiber mats and to measure the mass of absorbed resin and the rate of absorption. A good theoretical approximation was also obtained for describing the resin absorbency of glass fiber mats. It was found that there is a linear relationship between the pore sizes estimated with the help of the statistic fiber mat model and the uptake rate.

*Keywords:* glass fiber mat, resin absorbency.

## 1. Introduction

Polymer composites consisting of a matrix and reinforcement are more and more frequently used as structural materials. The reinforcing material is usually glass or carbon fiber, and the importance of natural and basalt fibers also increases, while the matrix is generally a kind of resin. In case of large surfaces or laminated composite plates glass fiber mats are often applied [1]. In order to provide a strong adhesion between the matrix and the reinforcement the latter should be soaked with the resin, hence the quality of the reinforcing effect depends on the interaction between the two elements [2].

During our experiments glass fiber mats that are most often used in Hungary were tested. The average value of pores and their distribution function were estimated using the mat statistic model and the measured geometrical parameters [3]. Pore size influences the absorbance process and the absorbed quantity of resin during composite production when the resin is still in a liquid phase [4]. A reproducible measurement and evaluation method was developed in order to compare the absorbency properties of glass fiber mats of the same specific weight but bonded in different ways (powder, emulsion). The relation between the resin absorption process characteristics and the structural properties of fiber mats was investigated using the theoretical considerations and the measurement results. The main aim was to measure and evaluate the absorption ability of resins in glass fiber mats.

## 2. Experimental

### 2.1. Materials

The polyester resin applied in the measurements was Viapal VUP 4627 BEMT/56 type provided by Novia.

The glass fiber mats (GFM) used were provided by Novia Kft, Hungary and their nominal data are summarized in *Table 1*. The fiber mats can be bound chemically with two different bonding agents, either powder or emulsion.

*Table 1.* Nominal data of glass fiber mats

Glass fiber mat sample	GFM1	GFM2	GFM3
Nominal fiber diameter ( $\mu\text{m}$ ) – $d_0$	12.5	12	12
Linear density of the roving (tex) – $q_0$	25	30	30
Length of the chopped roving(mm) – $l$	50	50	50
Bonding agent	Polyester powder GFM1P Emulsion GFM1E	Polyester powder GFM2P Emulsion GFM2E	Polyester powder GFM3P
Surface mass of the mat ( $\text{g}/\text{m}^2$ ) – $Q_0$	450	450	450
Mat standard width (cm)	125	125	125
Density of E-glass ( $\text{g}/\text{cm}^3$ ) – $\rho$	2.6	2.6	2.6
Producer	Johns Manville	Scottbader	Ahlstrom

The powder bonding agent is made of polyester powder that is well-soluble in polyester resin, hence mats bonded this way are usually used in manual lamination. The bonding agent of emulsion GFMs is polyvinyl acetate and this type of mat is used in continuous processes [5].

### 2.2. Methods

#### 2.2.1. Viscosity Measurement of Resins

The viscosity of the polyester resin used is a very important characteristic since it influences the resin absorbance capability of the fiber mat. Only a range of viscosity is given among the product data of resins but exact data are necessary for studying how resin viscosity affects the absorbency of mats.

The measurements were carried out on a Rheo-Viskometer at the Department of Plastics and Rubber Technology, BME. The method is the following: a cuvette of given length is filled with resin and a glass ball of given diameter immerses in it. Viscosity is derived from the resistance against the resin. The time when the ball sinks 30 mm deep in the cuvette is measured.

### 2.2.2. Geometrical Properties of Fibers

The diameters of 100 single fibers ( $d_0$ ) were measured with a Projectina projection microscope and an image analysis system [6, 7]. Programme Yarn\_93, developed in cooperation with KFKI, Research Institute for Technical Physics and Materials Science, was used in the measurements. The measurement principle was that inflection points of the gray level distribution histogram were determined from the outer part of the curve and contour width ( $W \approx d_0$ ) was measured. This is illustrated in Fig. 1.

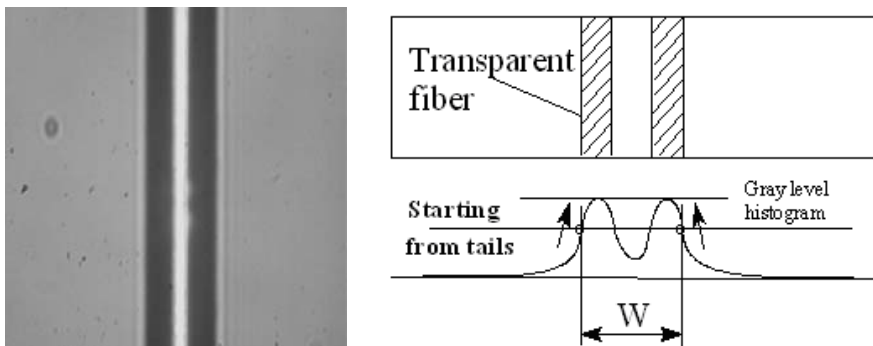
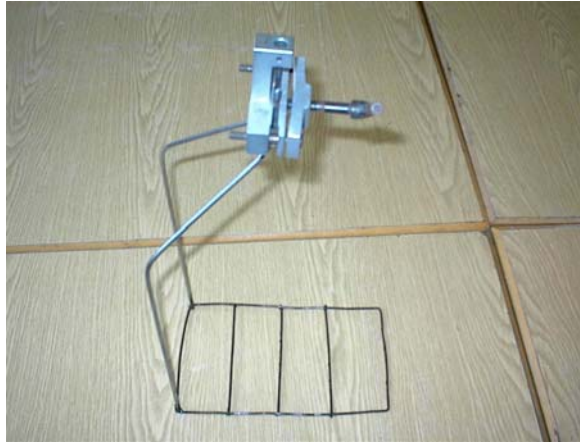


Fig. 1. Micrograph of a single glass fiber and the illustration of fiber diameter determination

The length ( $l$ ), width ( $a$ ) and thickness ( $b$ ) of the fibers gained from the mats were determined with a length measuring device, while mass ( $m$ ) was measured on analytical scales.

### 2.2.3. Method of Liquid Absorption

A welded steel frame (see Fig. 2) was prepared for this purpose and the glass fiber mat was placed on it.



*Fig. 2.* Welded steel frame

The measurement was carried out on a Zwick 1464 tensile tester, with the help of which the force that comes from the mass can be read. The measurement process is the following: the fiber mat sample is immersed in the resin and then lifted and this is repeated until the sample becomes saturated. The time of reading the force was 10 s in case of quickly saturating samples and 20, 30, 40 and 60 s in case of slower absorption processes.

### 3. Theory

#### 3.1. Theory of Pore Size Determination

Pore size, i.e. the diameter of the circle that can be inscribed in the voids among fibers, is a characteristic of the fiber structure (that of a glass fiber mat is illustrated in *Fig. 3*) and determines the liquid absorbance properties of the glass fiber mat.

If the center lines of fibers are considered, a virtual pore can be defined but if the thickness of the fibers is not neglected real pore dimensions are obtained. The explanation of these pores can be seen in *Fig. 4*.

The formula below gives a way to determine  $K$ , fiber centroid density [2]:

$$q_0 K n l = Q_\infty \quad (1)$$

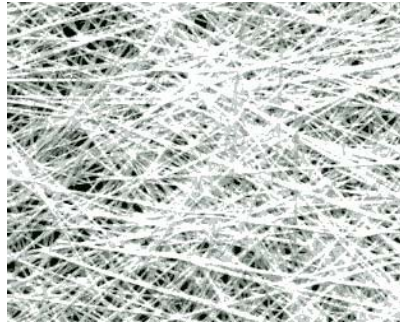


Fig. 3. Illustration glass fiber mat structure

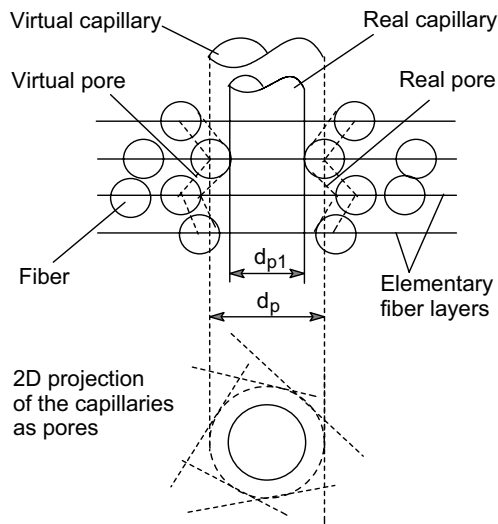


Fig. 4. Interpretation of pores in a glass fiber mat

where

- $Q_\infty$  is the average surface density,
- $q_0$  is fiber linear density,
- $n$  is the expected value of the number of elementary fibers in the roving, while
- $l$  denotes the expected value of roving length.

The value of the characteristic fiber number,  $n_0$ , i.e. the number of fiber centroids that fall into a radius around the fiber centroid:

$$n_0 = 2Kl^2/\pi \tag{2}$$

The value of  $E(\rho_0)$ , i.e. the expected pore radius, can be determined with the help of a standard normal distribution [2]:

$$E(\rho_0) = \frac{e^{-\frac{n_0}{2}}}{\sqrt{K}} [1 - \Phi(\sqrt{n_0})] = g(n_0) \quad (3)$$

If  $n_0 \geq 1$  an upper estimation is obtained for  $E(\rho_0)$  due to the exponential characteristic of the density function:

$$E(\rho_0) \leq \frac{1}{2Kl} = E(\rho_0)_{\max} \quad (4)$$

Virtual pore diameter ( $d_p$ ) can be determined from the expected value of the pore radius:

$$d_p = 2E(\rho_0)_{\max} \quad (5)$$

### 3.2. Model of Liquid Absorption

Liquid absorbency processes usually follow the curve shown in Fig.5. On this basis a liquid mass that is absorbed in infinite time can be determined. This is referred to as saturated mass. Since measurements are carried out in a given time interval, time  $t_T$  and a correspondent  $m_T$  can be defined.

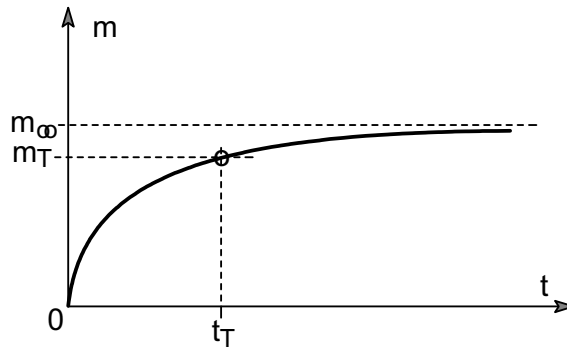


Fig. 5. Liquid absorption diagram

Liquid absorption processes in fibrous structures can be described with the help of the Lucas-Washburn formula [8]:

$$\frac{dh}{dt} = \dot{h} = \frac{b}{h} - a \quad (6)$$

where

$h$  is the height of the meniscus,  
 $t$  denotes time,  
 $a$  and  $b$  are constants,

defined in the following expressions:

$$a = \frac{r^2 \rho g}{8\eta} \quad (7)$$

$$b = \frac{r \gamma \cos \theta}{4\eta} \quad (8)$$

where

$r$  is the radius of pore or capillary,  
 $g$  is gravitational acceleration ( $g = 9.81 \text{ m/s}^2$ ),  
 $\gamma$  is surface tension,  
 $\rho$  and  $\eta$  are the density and viscosity of the liquid  
 $\theta$  is the contact angle between the liquid and the sample.

If the mass ( $m$ ) or weight ( $w$ ) of the liquid is measured, the following formula is valid for the meniscus height:

$$m = hA\rho \quad (9)$$

$$w = mg \quad (10)$$

In the initial and last phase of liquid absorption process the Washburn equation takes the following simplified form [9]:

$$\frac{dh}{dt} = \frac{b}{h} \quad (11)$$

the solution of which for the initial phase is:

$$h(t) = \sqrt{2bt} = k\sqrt{t} \quad (12)$$

where  $k$  is a constant.

The initial Washburn equation is integrated and transformed on the basis of (6) and the following implicit form is obtained [10]:

$$\frac{at}{h_\infty} = \ln \frac{1}{1 - \frac{h(t)}{h_\infty}} - \frac{h(t)}{h_\infty}. \quad (13)$$

The modified explicit solution that has asymptotically exact solutions for both  $t \rightarrow 0$  and  $t \rightarrow \infty$  is:

$$\frac{h(t)}{h_\infty} = \left[ 1 - e^{-\left(\frac{2at}{h_\infty}\right)^{\frac{1}{k}}} \right]^{\frac{1}{n}}, \quad (14)$$

and related to mass (Fig. 5):

$$m(t) = m_\infty \left[ 1 - e^{-\left(\frac{2a_m \cdot t}{m_\infty}\right)^{\frac{1}{k}}} \right]^{\frac{1}{n}}, \quad (15)$$

where the following condition must be fulfilled:

$$nk = 2 \quad (16)$$

## 4. Results

### 4.1. Viscosity Measurements

The measurement results summarized in *Table 2* are obtained with the help of the following simple *Eq. 17* found in the device manual:

$$\eta = K \cdot t \cdot p [\text{mPas}] \quad (17)$$

where

- $K$  is the cuvette constant (in this case  $K=0.1$ ),
- $t$  is the time during which the measuring ball immerses 30 mm deep into the resin in the cuvette [s],
- $p$  denotes loading [ $\text{p}/\text{cm}^2$ ].

The most optimal value of viscosity is where the immersion time is closest to 30 seconds. This condition is realized when  $p=100$ , hence most measurements were carried out under this loading and viscosity was considered to be  $\eta \sim 290$  [mPas] at 20°C room temperature (see the first row in *Table 2*).

### 4.2. Geometrical Properties of Fibers

The mean, minimum and maximum values of the single fiber diameters were examined and standard deviation as well as relative deviation were determined. These



Table 2. Measured viscosity

Time ( $t$ ) [s]	Loading ( $\rho$ ) [p/cm <sup>2</sup> ]	Viscosity ( $\eta$ ) [mPas]
28.9	100	288.7
31.8	90	286.4
26.1	110	287.1
22.9	120	274.9
34.5	80	276.4
27.2	100	272.0
27.4	100	274.3

values were compared to the nominal values and the difference was not more than 2% (see Table 3). The linear density of the single fiber ( $q_0$ ) can be determined if

Table 3. Fiber diameter data (measured and nominal)

$d_0$	Nominal [ $\mu\text{m}$ ]	Measured [ $\mu\text{m}$ ]	Min [ $\mu\text{m}$ ]	Max [ $\mu\text{m}$ ]	St. deviation [ $\mu\text{m}$ ]	Relative deviation
GFM1P	12.5	12.51	9.80	15.23	1.03	0.083
GFM2P	12	12.14	9.43	15.00	1.26	0.104
GFM3P	12	11.97	9.27	14.57	1.15	0.096
GFM1E	12.5	12.46	9.80	15.07	1.15	0.092
GFM2E	12	12.29	9.40	14.97	1.23	0.100

the density ( $\rho$ ) and the measured diameter ( $d_0$ ) of E-glass fibers are known using the following equation, where  $d_0 \approx W$ :

$$q_0 = \rho A = \rho \frac{d_0^2 \pi}{4} \quad (18)$$

The number of single fibers ( $n$ ) in a roving was determined in two different ways (the results are summarized in Table 4).

First of all, the value of  $n_1$  can be determined using the average linear density and the average length of fibers:

$$q_1 = \frac{m_i}{l_i} \quad (19)$$

$$n_1 = \frac{q_1}{q_0} \quad (20)$$

Then a less accurate way is to use the width ( $a$ ) and thickness ( $b$ ) of rovings and to determine how many fibers can fit theoretically in this territory ( $a \times b$ ). This method was used for checking since the previous method gives a better estimation.

$$n_2 = \frac{a_i \cdot b_i}{A_0} = \frac{a_i \cdot b_i}{\frac{d_0^2 \pi}{4}} \quad (21)$$

$$q_2 = n_2 q_0 \quad (22)$$

Table 4. Number of fibers in GFMs ( $n$ )

	$l$ [mm]	$a$ [mm]	$b$ [mm]	$m$ [g]	$n_1$	$n_2$	$ n_1/n_2 $
GFM1P	50.39	0.44	0.033	0.0019	134.34	129.52	0.964
GFM2P	49.68	0.40	0.043	0.0023	163.69	160.48	0.980
GFM3P	50.11	0.34	0.043	0.0020	141.61	133.05	0.940
GFM1E	48.53	0.27	0.047	0.0017	122.54	116.10	0.947
GFM2E	49.07	0.44	0.061	0.0034	208.51	217.58	0.958

The two methods show higher accordance than 94 %.

The average pore diameter can be calculated based on (5) and its values are summarized in Table 5.

Table 5. Average pore size in glass fiber mats

	$K$ [1/cm <sup>2</sup> ]	$n_0$	$d_p$ [μm]
GFM1P	23.83	385.28	83.26
GFM2P	19.78	310.80	101.94
GFM3P	23.11	369.37	86.35
GFM1E	27.46	411.72	75.04
GFM2E	13.16	201.78	154.82

The average pore diameter in sample GFM2E is significantly higher than the other. The cause of this difference lies in the structure of the mat that should be studied further.

### 4.3. Liquid Absorption of Glass Fiber Mats

The graphs show the weight of the absorbed resin related to the weight of glass fiber mat (Fig. 6). The saturating time of glass fiber mats ( $t_T$ ), the maximal absorbed resin

weight ( $m_T$ ) related to the weight of the glass fiber mat ( $m_0$ ) and the correspondent relative saturating time ( $k_T/m_0$ ) are summarized in *Table 6*.

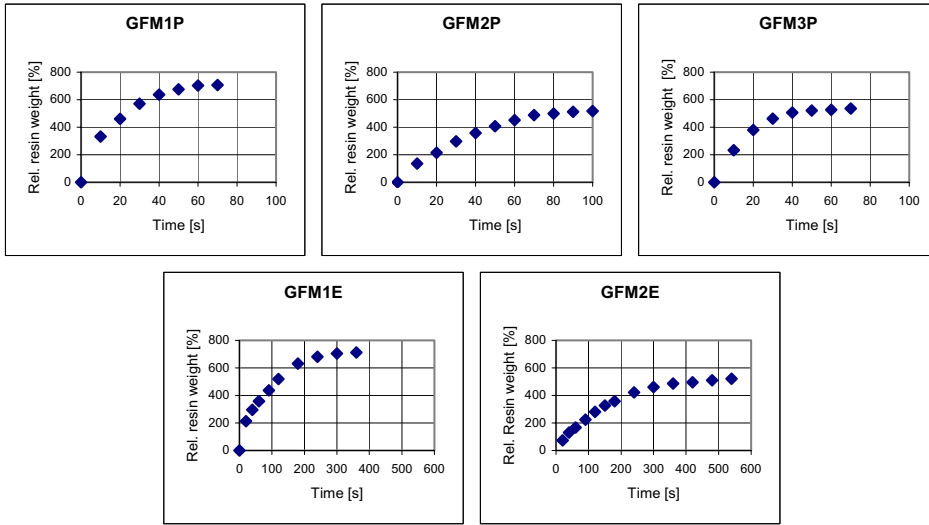


*Fig. 6.* Resin absorption of glass fiber mats as a function of time

In order to determine the speed of saturation the absorbed relative resin weight ( $m_T/m_0$ ) is graphed as a function of the square root of time ( $\sqrt{t_T}$ ) in *Fig. 7*. The explicit solution of the simplified Washburn equation for the initial phase:

$$\frac{m_T}{m_0} = \frac{k_T}{m_0} \sqrt{t_T} \tag{23}$$

where  $k_T$  is the saturation value of  $k$  already defined.

The  $k_T/m_0$  constants can be determined from the diagrams in *Fig. 7*, since they are the same as the steepness of the trendlines ( $y$ ). The resin absorbency characteristics of the different mats can be analysed and compared in *Table 6*.

#### 4.3.1. Theory Fitting

Evaluation of resin absorbency with the help of the explicit form of the Washburn equation, and the initial part of the curve have been approximated with a tangent. The solution has been reached through steps of iteration. Since the curves did not start from the origin (*Fig. 8*), the diagrams were shifted along the time axis.

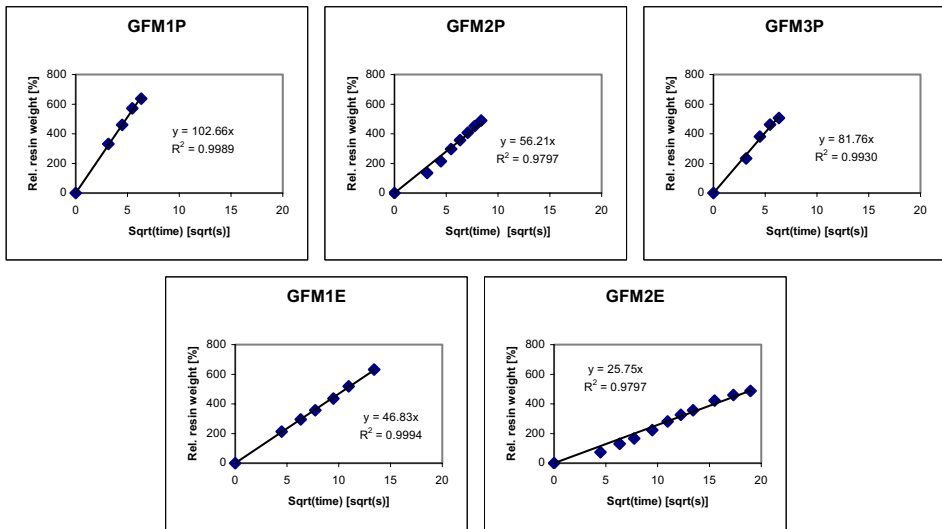


Fig. 7. The initial phase of resin absorbency as a function of the square root of time

Table 6. Characteristics of resin absorbency

	$k_T/m_0 = y$ [%/sqrt(s)]
GFM1P	46.83
GFM2P	56.21
GFM3P	81.76
GFM1E	102.66
GFM2E	25.75

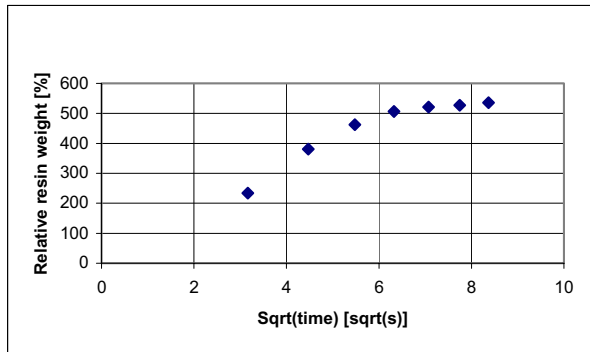


Fig. 8. Initial part of resin uptake (example of GFM3P)

The correction of the initial part of the curve was carried out on 3 points in case of the quickly saturating powder bonded mat, and 6 points in case of the slowly saturating emulsion bonded mats. The time axis was shifted with an adequate value  $(t_0) \cdot k'_0$  initial tangent steepness was determined from the diagram in Fig.9 (Table 7). The initial tangent compared to the whole process is illustrated in Fig. 10.

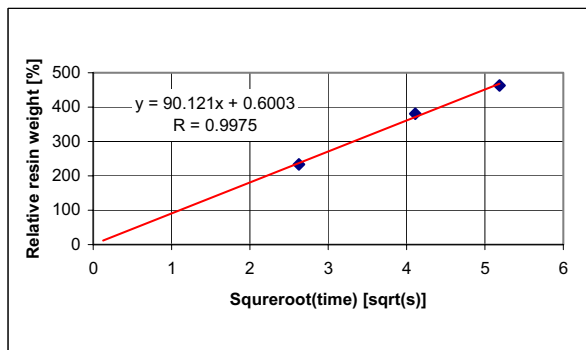


Fig. 9. Fitting a line to the initial part of resin absorption with zero point shift (example of GFM3P)

Table 7. Shift values ( $t_0$ ) and the steepness of the initial tangent ( $k_0'$ )

	$t_0$ [s]	$k_0'$
GFM1P	0.9	103.52
GFM2P	4.8	59.38
GFM3P	3.1	90.12
GFM1E	0.6	47.12
GFM2E	11.5	27.09

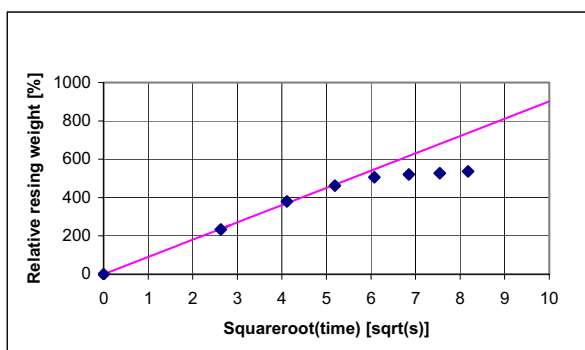


Fig. 10. Initial tangent compared to the total data series (example of GFM3P)

Since the measured results (see e.g. Fig. 6) are related to mass  $m_0$ , Eq. (15) was transformed in the following way:

$$w(t) = w_\infty \left[ 1 - e^{-\left(\frac{2a_0 \cdot t}{w_\infty}\right)^{\frac{1}{k}}} \right]^{\frac{1}{n}} \quad (24)$$

where

$$w(t) = \frac{m(t)}{m_0} \quad (25)$$

$$a_0 = \frac{a}{m_0} \quad (26)$$

for the initial part:

$$w(t) \approx k_0\sqrt{t} \tag{27}$$

where

$$k_0 = \sqrt{2b_0} \tag{28}$$

$$b_0 = \frac{b}{m_0^2} \tag{29}$$

then the value of  $w_\infty$  was estimated from Fig. 6 for each glass fiber mat. The  $p = 1/k$  exponent was chosen and the scale parameters of the explicit approximation were determined. On the basis of Eq. (15) a curve is fitted on the measured

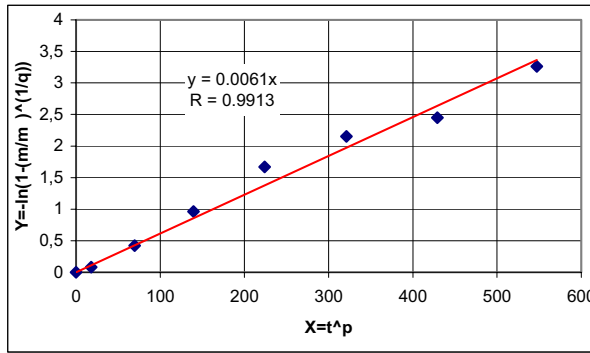


Fig. 11. Fitting the explicit Washburn equation and the determination of constant C example of GFM3P)

points then the relative average square error of the measured and estimated value (RASE%) was calculated in the following way: the value of  $w_\infty$  was changed at fixed  $p = 1/k$ , the final value was changed until the relative square error became minimal (if possible, a minimal value of  $S\%RASE\%$  is also realized).  $S\%$  is a deviation-like quantity and is calculated in the following way:

$$S\% = 100 \cdot \sqrt{1 - R^2} \tag{30}$$

where  $R$  is the correlation coefficient in Fig. 11.

A curve was obtained this way for the saturation processes that gives a smaller RASE% value than 2% and provides a good approximation for the measurement. The average error ( $S\% \cdot RASE\%$ ) of the approximation process is shown as a function of the final value in Fig. 12. Table 8 reveals the results of the calculations of the best iteration of the above mentioned quantities including  $k_0$ , the resin uptake rate as well.

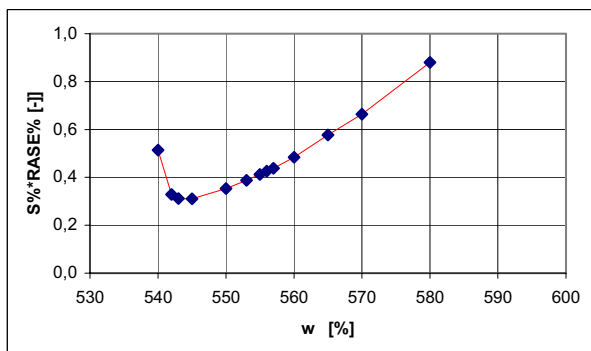


Fig. 12. Fitting optimization with fix exponents (example of GFM3P)

Table 8. Parameters of fitting the explicit Washburn equation

	$w_{\infty}$	$p = 1/k$	$k_0$	RASE%	$b_0$	$a_0$	$\text{sqrt}(a_0)$
GFM1P	725	2.0	108.41	1.43	5877	8.11	2.85
GFM2P	520	7.0	61.30	1.13	1879	3.61	1.90
GFM3P	543	1.5	99.21	1.95	4922	9.06	3.01
GFM1E	720	2.4	48.59	1.75	1180	1.64	1.28
GFM2E	522	7.0	27.68	1.80	383	0.73	0.86

Fig. 13 illustrates the results of the estimation process, where the initial approximation was made according to (25), while the global one on the basis of Eq. (23).

The relation between the structural characteristics of glass fiber mats and the parameters was determined during resin absorption. Since average pore diameter ( $d_p$ ) characterizes mats well, this value was compared to resin uptake rate ( $k_0$ ) in Table 9. It can be concluded that the smaller the average pore size, the faster the resin uptake is. This phenomenon can be explained with the capillary effect.

## 5. Conclusions

The method worked out for resin uptake can be used to model the liquid absorbance process of glass fiber mats and to measure the mass of absorbed resin and the rate of absorption as revealed in Fig. 13.

A good theoretical approximation was obtained for describing the absorbed resin mass values using the evaluation process based on the Washburn equation. As a result a linear relationship was experienced between the pore sizes ( $d_p$ ) estimated



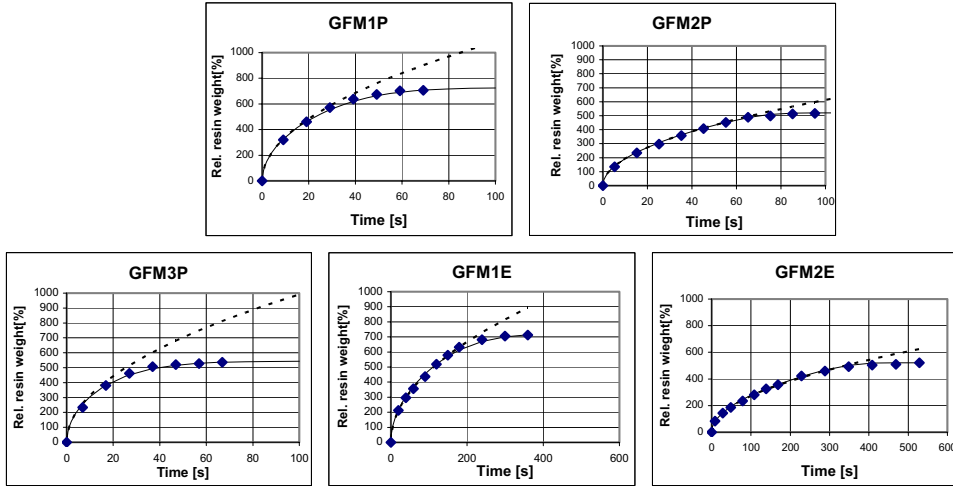


Fig. 13. Measured (◆) and estimated (initial estimation: dotted line; global estimation full line) processes of resin uptake for each mat

Table 9. Average pore diameter and resin uptake comparison

	$d_p$ [ $\mu\text{m}$ ]	$k_0$ [%/square root(s)]
GFM1P	83.26	108.41
GFM2P	101.94	61.30
GFM3P	86.35	99.21
GFM1E	75.04	48.59
GFM2E	154.82	27.68

with the help of the statistic fiber mat model and the uptake rate ( $k_0$ ) proportional to the hydraulic pore diameter according to Washburn.

It can also be concluded that the smaller the average pore size, the faster the resin uptake is, due to the capillary effect.

### Acknowledgement

The authors would like to thank Novia Kft. for the materials. The research was funded by application OTKA T038220.

## References

- [1] CZVIKOVSKY, T.– NAGY, P. – GAÁL, J., The Basics of Polymer Engineering (in Hungarian: A polimerteknika alapjai), Műegyetemi Kiadó, Budapest, 2000.
- [2] HÓRVÖLGYI, Z., Physical-Chemical Characterization of 3P Resins and Resin Components: Rheological Properties and Wettability (in Hungarian: A 3P gyanták és gyantakomponensek fizikai-kémiai jellemzése: reológiai tulajdonságok és nedvesítő képesség), *Műanyag és Gumi*, 2004. **41**, 8. szám, p. 315.
- [3] VAS, L. M., Design of Textile Products – Structural and Macroproperties (in Hungarian: Textiltermékek tervezése- Szerkezeti és makrotulajdonságok), manuscript, Budapest, 2000.
- [4] NAGY, V. – KOSTAKOVA, E. – VAS, L. M., Investigation of Porosity in Polyester Staple Yarns. *5th International Conference TEXSCT03, Textile Science 2003*; Liberec, CZ, Proceedings, pp. 164–167.
- [5] SCHWARZ, O., Glasfaserverstärkte Kunststoffe – Kurz und Bündig Verarbeitung von Glasfaserverstärkten Kunststoffen Kamprath – Reihe Kurz und Bündig by Vogel-Verlag, Würzburg (Deutschland).
- [6] RAHEEL, M. (edited by): *Modern Textile Characterization Methods*, Marcel Dekker, Inc. New York, 1996.
- [7] GYIMESI, J., Physical Testing of Textile Materials (in Hungarian: Textilanyagok fizikai vizsgálata), Műszaki Könyvkiadó, Budapest, 1968.
- [8] DUTKIEWICZ, J., Some Advances in Nonwoven Structures for Absorbency, Comfort and Aesthetics, *Autex Research Journal*, **2**, No. 3. (2002).
- [9] WASHBURN, E. W., The Dynamics of Capillary Flow, *The Physical Review*, March 1921, **17**, No. 3.
- [10] NAGY, V.– VAS, L. M., Testing Liquid Absorption in Polyester Staple Yarn. *Fibres & Textiles in Eastern Europe*, 2005, under submission.